How to cite: *Angew. Chem. Int. Ed.* **2023,** *62,* e202215894
International Edition: doi.org/10.1002/anie.202215894
German Edition: doi.org/10.1002/ange.202215894

Photoreforming Catalysts

Comproportionation of CO_2 and Cellulose to Formate Using a Floating Semiconductor-Enzyme Photoreforming Catalyst

*Erwin Lam, Melanie Miller, Stuart Linley, Rita R. Manuel, Inês A. C. Pereira, and Erwin Reisner**

Abstract: Formate production via both CO_2 reduction and cellulose oxidation in a solar-driven process is achieved by a semi-artificial biohybrid photocatalyst consisting of immobilized formate dehydrogenase on titanium dioxide (TiO_2|**FDH**) producing up to 1.16 ± 0.04 $mmol_{formate}\, g_{TiO_2}^{-1}$ in 24 hours at 30 °C and 101 kPa under anaerobic conditions. Isotopic labeling experiments with ^{13}C-labeled substrates support the mechanism of stoichiometric formate formation through both redox half-reactions. TiO_2|**FDH** was further immobilized on hollow glass microspheres to perform more practical floating photoreforming allowing vertical solar light illumination with optimal light exposure of the photocatalyst to real sunlight. Enzymatic cellulose depolymerization coupled to the floating photoreforming catalyst generates 0.36 ± 0.04 $mmol_{formate}$ per m^2 irradiation area after 24 hours. This work demonstrates the synergistic solar-driven valorization of solid and gaseous waste streams using a biohybrid photoreforming catalyst in aqueous solution and will thus provide inspiration for the development of future semi-artificial waste-to-chemical conversion strategies.

Sunlight-driven chemical transformations represent a sustainable route to mitigate waste streams and produce value-added chemicals.[1] For example, the greenhouse gas CO_2 can be converted to valuable fuels or chemical feedstocks in the presence of a suitable semiconductor.[2,3] The photocatalyst absorbs light to generate photo-excited electrons that perform a reduction reaction such as CO_2 conversion to CO or formate ($HCOO^-$).[4–6] The holes remaining in the semiconductor regenerate through oxidation of H_2O to O_2 in artificial photosynthesis.[4,7,8]

[*] E. Lam, M. Miller, S. Linley, E. Reisner
Yusuf Hamied Department of Chemistry, University of Cambridge
Lensfield Road, CB2 1EW, Cambridge (UK)
E-mail: reisner@ch.cam.ac.uk
R. R. Manuel, I. A. C. Pereira
Instituto de Tecnologia Química e Biológica António Xavier (ITQB NOVA), Universidade NOVA de Lisboa
2780-157 Oeiras (Portugal)

Photoreforming (PR) provides an alternative to O_2 evolution by oxidizing waste substrates into valuable organics instead.[9–12] Waste oxidation through PR has mainly been performed in combination with proton reduction to H_2. Achieving CO_2 photoreduction combined with waste photooxidation would take advantage of both the reduction and oxidation half-reactions in photocatalysis and generate valuable carbon-based products from each. Additionally, PR of glucose, for example, avoids O_2 evolution, thereby requiring less thermodynamic driving force ($\Delta G^\circ = -35$ kJ mol^{-1} vs. 237 kJ mol^{-1} for water splitting).

TiO_2 represents an archetypical PR catalyst that can perform solar-driven oxidation of biomass coupled to the reduction of protons to H_2,[13,14] using co-catalysts such as Pt or MoS_2 to enhance photocatalytic activity.[15,16] We have previously reported an example that combines CO_2 reduction with waste oxidation by using a phosphonate group-bearing molecular cobalt(II)terpyridine complex anchored on TiO_2 (TiO_2|**CotpyP**), reducing CO_2 to CO while oxidizing pre-treated cellulose to $HCOO^-$.[17]

Conveniently, CO_2 can also be reduced to $HCOO^-$, allowing for the possibility of combining CO_2 reduction with cellulose oxidation to generate $HCOO^-$ from both redox half-reactions through comproportionation. However, few co-catalysts are known that can selectively convert CO_2 to $HCOO^-$. A model catalyst for CO_2-to-$HCOO^-$ conversion is the enzyme formate dehydrogenase.[18,19] Most studies with formate dehydrogenase use the metal-independent enzymes that require NADH as electron donor.[20] In nature, these enzymes do not operate for CO_2 reduction, as this reaction is thermodynamically unfavorable,[21] and is only achieved in vitro at low rates (≈ 0.01 to 1 s^{-1})[22,23] by the use of high concentrations of NADH, which is unstable and expensive.[24] In contrast, metal-dependent formate dehydrogenases, which can have molybdenum or tungsten (W) at the active site, present CO_2 reduction activities orders of magnitude higher than metal-independent ones (≈ 10 to 400 s^{-1}). This is made possible by receiving electrons directly from an exogenous donor which are transferred to the active site through a chain of iron-sulfur clusters.[18,19,25] Such a W-dependent formate dehydrogenase (W/Sec-formate dehydrogenase from *Desulfovibrio vulgaris* Hildenborough (*Dv*H W/Sec-FDH_{AB}; denoted as **FDH**) has previously been interfaced with TiO_2 to selectively drive the photo-conversion of CO_2-to-$HCOO^-$ in the presence of the sacrificial electron donor triethanolamine.[26] Systems for electrocatalytic comproportionation of CO_2 and solid plastic waste have been demonstrated,[27] but a related enzyme-hybrid

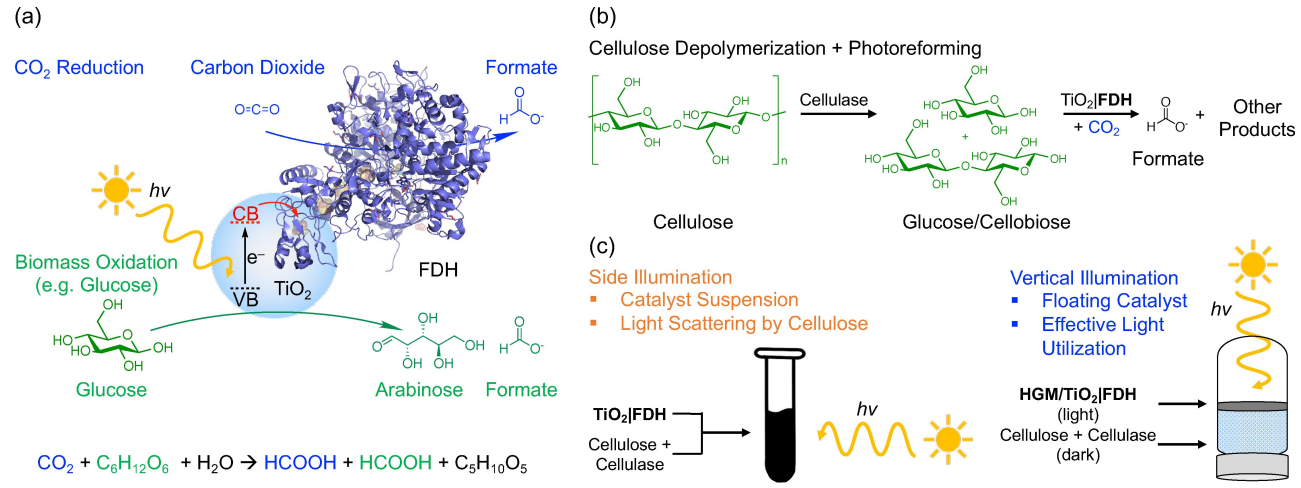

Figure 1. a) Photoreforming using TiO_2|**FDH** for selective CO_2-to-$HCOO^-$ reduction coupled to glucose-to-$HCOO^-$ and arabinose oxidation, demonstrating the possibility of photocatalytic comproportionation to form a single energy carrier from both half-reactions. b) Pre-treatment of cellulose with cellulase to generate soluble glucose and cellobiose for photoreforming forming $HCOO^-$ with CO_2 and TiO_2|**FDH**. c) Suspended TiO_2|**FDH** for side irradiation (left) and floating **HGM/TiO_2**|**FDH** (right) for top-down solar light irradiation combined with cellulose depolymerization for $HCOO^-$ formation.

photocatalyst system has not yet been reported for PR. This is due to several challenges that include finding compatible reaction conditions and co-catalysts suitable for both redox half-reactions.

Here, we report simultaneous photocatalytic conversion of CO_2 and cellulose to $HCOO^-$ enabled by a selective photocatalyst consisting of an immobilized **FDH** on TiO_2 (TiO_2|**FDH**) (Figure 1a). The TiO_2|**FDH** photocatalyst oxidizes sugars or enzyme pre-treated cellulose to $HCOO^-$ while reducing CO_2-to-$HCOO^-$ (Figure 1b). This system manages to perform CO_2-to-$HCOO^-$ conversion without the requirement of costly NADH,[28–30] where electrons are provided through oxidation of waste substrates (e.g. cellulose) and channeled to **FDH** through TiO_2 acting as a light absorbing semiconductor. Additionally, a practical floating TiO_2|**FDH** photocatalyst allows photocatalytic $HCOO^-$ formation while soluble sugar-based electron donors are simultaneously generated in the dark through enzymatic cellulose depolymerization (Figure 1c).

The photocatalytic activity of **FDH** immobilized onto TiO_2 for CO_2 reduction with glucose as the electron donor was first investigated (Figure 2a and Table S1). A 20 μM solution of **FDH** in 20 mM tris(hydroxymethyl)aminomethane (Tris) buffer at pH 7.5 was activated with DL-dithiothreitol (DTT, 25 mM) under anaerobic conditions.[19,31] The activated **FDH** (14.5 $nmol_{\mathbf{FDH}}\,g_{TiO_2}^{-1}$) solution was added to a glass photoreactor containing an aqueous TiO_2 suspension (0.83 $mg\,mL^{-1}$, P25, particle diameter ~20 nm) in 0.1 M $NaHCO_3$ and 0.1 M D(+)-glucose at pH 6.5 for self-immobilization. The sealed glass reactor was irradiated through side illumination with a solar light simulator (100 $mW\,cm^{-2}$, AM 1.5G, 30 °C and 101 kPa) for 24 h while stirring. Analysis of the liquid products showed the formation of $0.96\pm0.05\ mmol_{formate}\,g_{TiO_2}^{-1}$ (by ion chromatography) and $0.47\pm0.06\ mmol_{arabinose}\,g_{TiO_2}^{-1}$ (by high performance liquid chromatography) while no (or only small amounts of) CO and H_2 ($<0.04\ mmol\,g_{TiO_2}^{-1}$) were detected by gas chromatography (Figure 2a). The formation rate of

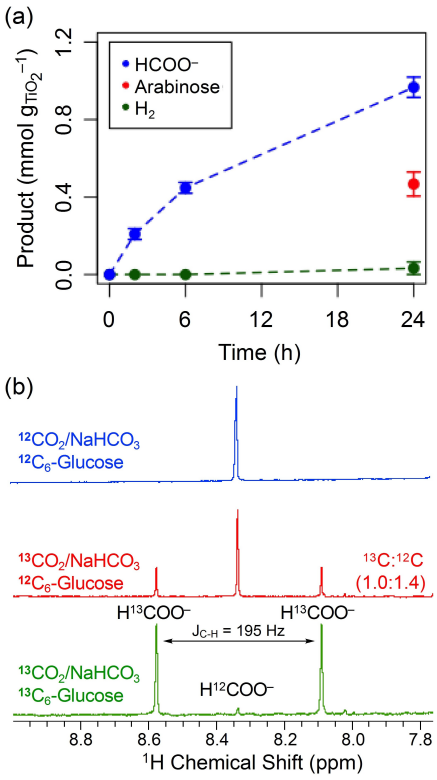

Figure 2. a) Formate, arabinose and H_2 formation with TiO_2|**FDH**. b) Formate detection by ^1H NMR spectroscopy (D_2O) of the reaction solution after photocatalysis with ^{13}C-labeled $^{13}CO_2$/$NaHCO_3$ and/or $^{13}C_6$-glucose. $H^{13}COO^-$ is indicated by a $J_{C\text{-}H}$ coupling induced doublet (195 Hz) of formate. Reaction conditions: 0.83 mg TiO_2; 12 nM **FDH**; 0.1 M glucose; 0.1 M $NaHCO_3$; pH 6.5; 1 mL; anaerobic atmosphere; 30 °C; 101 kPa.

$HCOO^-$ was significantly reduced from 6 to 24 h photocatalysis (Figure 2a), showing the limited stability of **FDH**, consistent with previous photocatalysis work with **FDH**.[26]

Isotopic labeling experiments were performed with ^{13}C-labeled $^{13}CO_2/NaH^{13}CO_3$ and $^{13}C_6$-glucose (Figure 2b, blue trace for the unlabeled experiment). After 24 h photocatalysis and analysis of the reaction solution by ^1H NMR spectroscopy, only $H^{13}COO^-$ was formed indicated by the presence of a doublet induced by $J_{C\text{-}H}$-coupling (195 Hz) between the ^{13}C-carbon (spin = 1/2) and the ^1H of $H^{13}COO^-$ (Figure 2b, green trace). A $^{12/13}C$ mixture of $CO_2/NaHCO_3$ and glucose ($^{13}CO_2/NaH^{13}CO_3$ and $^{12}C_6$-glucose (Figure 2b, red trace), or $^{12}CO_2/NaH^{12}CO_3$ and $^{13}C_6$-glucose (Figure S1, black trace) generated a mixture of $^{12/13}C$-$HCOO^-$, consistent with the formation of $HCOO^-$ from both redox half-reactions, with a $^{13}C:^{12}C$ ratio of 1.0:1.4 (Figure 2b, red trace).

Exclusion experiments in the absence of solar light irradiation, TiO_2 or glucose formed $< 0.14\ mmol_{formate}\ g_{TiO_2}^{-1}$ (Figure S2). In the absence of **FDH**, $0.98 \pm 0.05\ mmol_{formate}\ g_{TiO_2}^{-1}$ was formed along with $0.47 \pm 0.03\ mmol_{H_2}\ g_{TiO_2}^{-1}$ and $1.96 \pm 0.03\ mmol_{arabinose}\ g_{TiO_2}^{-1}$ (Figure S2). Without **FDH** as the co-catalyst, TiO_2 itself is an effective H_2 evolving photocatalyst under the employed conditions but does not catalyze any CO_2 reduction as confirmed by isotopic labeling experiments (Figure S3, black trace). In the absence of $CO_2/NaHCO_3$, $0.63 \pm 0.07\ mmol_{formate}\ g_{TiO_2}^{-1}$ and $0.39 \pm 0.06\ mmol_{arabinose}\ g_{TiO_2}^{-1}$ were formed (Figure S2). Although $HCOO^-$ was detected, it could only originate from glucose oxidation. Therefore, while $HCOO^-$, arabinose and H_2 were formed photocatalytically in the absence of **FDH** or $CO_2/NaHCO_3$, no CO_2 reduction to $HCOO^-$ occurred. Thus, all components in the photocatalytic system are required for simultaneous formation of $HCOO^-$ from both redox half-reactions.

The data from isotopic labeling and exclusion control experiments support that TiO_2 acts as a light absorber able to directly transfer its excited electrons to **FDH** where they combine with CO_2 and protons from the reaction solution to generate $HCOO^-$. The electron hole remaining in the valence band of TiO_2 is regenerated by the electron donor glucose, promoting its further conversion to arabinose and $HCOO^-$. In a typical CO_2-to-$HCOO^-$conversion by metal-independent formate dehydrogenases, NADH is required as a co-enzyme to supply protons and electrons for reduction. In this system, NADH is replaced by a light absorber that can directly inject electrons sourced from waste biomass into **FDH**, providing a low-cost, stable alternative to NADH desirable for effective use of **FDH**.

The product ratio after photocatalysis with $TiO_2|$**FDH** and glucose as the electron donor was ≈2:1 between $HCOO^-$ and arabinose (Figure 2a), consistent with selective conversion of CO_2 and glucose to $HCOO^-$ (Scheme S1). This was further supported by the $^{13}C:^{12}C$ ratio of $HCOO^-$ using $^{13}CO_2/NaH^{13}CO_3$ and $^{12}C_6$-glucose (see above), which was close to an expected stoichiometric reaction.

Photocatalysis with $TiO_2|$**FDH** ($14.5\ nmol_{FDH}\ g_{TiO_2}^{-1}$ and $0.83\ mg_{TiO_2}\ mL^{-1}$) and a decreased glucose concentration (0.01 M) resulted in the gradual formation of all reaction products leading to $0.90 \pm 0.02\ mmol_{formate}\ g_{TiO_2}^{-1}$ and $0.37 \pm 0.06\ mmol_{arabinose}\ g_{TiO_2}^{-1}$ after 24 h photocatalysis (Figure S4, S5 and Table S2). ^{13}C labeling experiments at 0.01 M glucose confirmed the conversion of $CO_2/NaHCO_3$ and glucose to $HCOO^-$ (Figure S6). Under optimized conditions ($14.5\ nmol_{FDH}\ g_{TiO_2}^{-1}$ and $0.83\ mg_{TiO_2}\ mL^{-1}$, 0.01 M glucose), the glucose to arabinose conversion yield was (3.1 ± 0.5)% after 24 h (Figure S4 and Table S2).

To explore the substrate scope, glucose was replaced with different soluble sugars for $HCOO^-$ formation: C_6-sugars (galactose, maltose, fructose), a C_5-sugar (arabinose) and a C_{12}-sugar (cellobiose) (Figure 3a and Table S3). In all cases, $HCOO^-$ was produced photocatalytically with $TiO_2|$**FDH**. C_6-sugars generated the most $HCOO^-$ ($\approx 1.00\ mmol_{formate}\ g_{TiO_2}^{-1}$ with galactose or mannose), similar to glucose ($0.96 \pm 0.05\ mmol_{formate}\ g_{TiO_2}^{-1}$). The formation of $HCOO^-$ from sugar oxidation can be explained by the

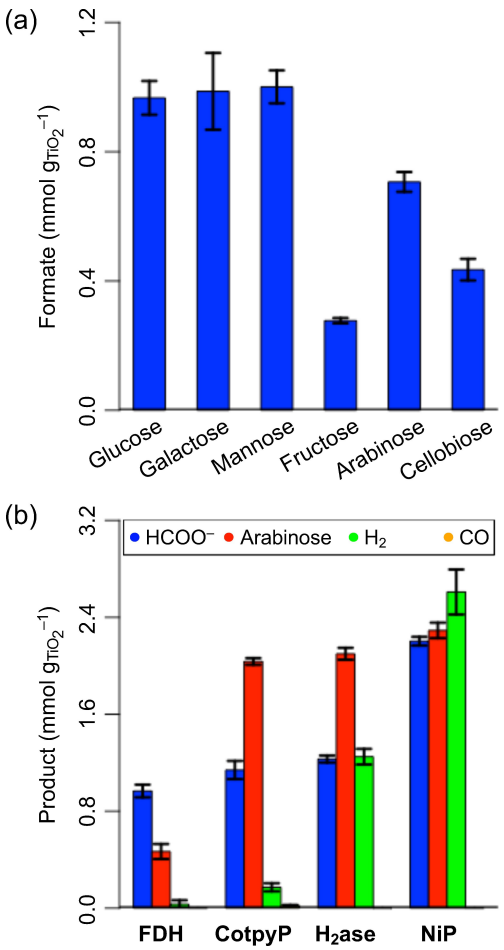

Figure 3. a) Formate formation after 24 h photocatalysis with $TiO_2|$**FDH** using different sugar-based electron donors. b) Formate, arabinose, H_2 and CO formation after 24 h photocatalysis combining TiO_2 with different molecular and enzyme co-catalysts and glucose as electron donor. Reaction conditions: a) 0.83 mg TiO_2; 12 nM **FDH**; 0.1 M donor; 0.1 M $NaHCO_3$; pH 6.5; 1 mL; anaerobic atmosphere; 30 °C; 101 kPa. b) 0.83 mg TiO_2; 12 nM enzyme (**FDH**, **H_2ase**) or 8.3 μM molecular catalyst (**CotpyP**, **NiP**); 0.1 M glucose; 0.1 M $NaHCO_3$; pH 6.5; 1 mL; anaerobic atmosphere; 30 °C; 101 kPa.

oxidation of the aldehyde functional group to a carboxylate followed by C–C bond cleavage forming $HCOO^-$, involving oxygen-centered radicals on TiO_2 formed during photocatalysis.[32,33] This mechanism is further supported by decreased $HCOO^-$ (0.28 ± 0.01 $mmol_{formate}\, g_{TiO_2}^{-1}$) formation with fructose, likely due to the absence of an aldehyde functional group. Arabinose and cellobiose showed lower amounts of $HCOO^-$ formed (0.71 ± 0.03 $mmol_{formate}\, g_{TiO_2}^{-1}$ and 0.43 ± 0.03 $mmol_{formate}\, g_{TiO_2}^{-1}$, respectively). Thus, the versatility of TiO_2|**FDH** to photoreform various types of sugars to $HCOO^-$ was shown.

We subsequently explored PR of TiO_2 with different molecular and enzyme co-catalysts. A molecular cobalt terpyridine co-catalyst (denoted as **CotpyP**) was selected for CO_2-to-CO reduction and a synthetic DuBois-type nickel bis(diphosphine) complex with solubilizing phosphate groups (denoted as **NiP**) as well as a hydrogenase from *Desulfovibrio vulgaris* Hildenborough (*Dv*H [NiFeSe]-H_2ase; denoted as **H_2ase**) (Figure S7) were chosen for proton reduction.

All co-catalysts were studied in PR for 24 h with glucose (0.1 M) as electron donor (0.83 $mg_{TiO_2}\, mL^{-1}$ with 8.3 μM **CotpyP** or **NiP**, or 12 nM **H_2ase**) (Figure 3b and Table S4). For TiO_2|**CotpyP**, 0.17 ± 0.03 $mmol_{H_2}\, g_{TiO_2}^{-1}$ and 0.023 ± 0.004 $mmol_{CO}\, g_{TiO_2}^{-1}$ along with 1.14 ± 0.08 $mmol_{formate}\, g_{TiO_2}^{-1}$ and 2.04 ± 0.03 $mmol_{arabinose}\, g_{TiO_2}^{-1}$ were formed. TiO_2|**CotpyP** mainly produced H_2 and only small amounts of CO. No $HCOO^-$ formed through CO_2 reduction with TiO_2|**CotpyP** indicated by ^{13}C-labeling (Figure S8). TiO_2|**H_2ase** generated 1.25 ± 0.06 $mmol_{H_2}\, g_{TiO_2}^{-1}$ along with 1.23 ± 0.03 $mmol_{formate}\, g_{TiO_2}^{-1}$ and 2.10 ± 0.05 $mmol_{arabinose}\, g_{TiO_2}^{-1}$. For TiO_2|**NiP**, 2.61 ± 0.19 $mmol_{H_2}\, g_{TiO_2}^{-1}$ along with 2.20 ± 0.04 $mmol_{formate}\, g_{TiO_2}^{-1}$ and 2.29 ± 0.06 $mmol_{arabinose}\, g_{TiO_2}^{-1}$ were formed.

PR with TiO_2 and various molecular and enzyme co-catalysts have comparable catalytic performances despite ≈1000 times lower co-catalyst loading for enzymes. Thus, the high product specificity and activity expected of enzymes was demonstrated, despite the presence of highly active radical species that could potentially deactivate the enzymes.[33] The current state-of-the-art molecular PR co-catalyst (**CotpyP**) has significantly lower activity and selectivity towards CO_2 reduction compared to **FDH** under these reaction conditions where CO_2 originates solely from its equilibrium with $NaHCO_3$. The product ratio for TiO_2|**H_2ase** deviates from what would be expected for a selective overall redox reaction, indicating the difficulty of controlling the overall reaction in PR conditions even for selective enzymes.

Thus far, different soluble sugars were used as model substrates for PR. We therefore sought to use insoluble biomass waste, such as polymeric cellulose. To fully utilize cellulose for PR, a pre-treatment step to solubilize cellulose to sugars must be implemented. One possibility is to use the enzyme cellulase to hydrolyze cellulose under ambient conditions in aqueous medium (Figure 1b). PR with TiO_2|**FDH** can conveniently be performed under similar conditions as enzymatic cellulose depolymerization, allowing for simultaneous pre-treatment and PR in an integrated process.

We performed PR experiments with TiO_2|**FDH** (12 nM **FDH**, 0.83 $mg_{TiO_2}\, mL^{-1}$) in 0.1 M $NaHCO_3$ at pH 6.5 in the presence of cellulose (16.2 $mg\, mL^{-1}$) and cellulase (0.8 $mg\, mL^{-1}$) (Figure 4a and Table S5). Cellulase depolymerized cellulose to cellobiose and glucose to act as soluble electron donors in the photooxidation step forming $HCOO^-$, while CO_2 was also reduced to $HCOO^-$. After 24 h of PR, 0.43 ± 0.02 $mmol_{formate}\, g_{TiO_2}^{-1}$ was formed along with glucose and cellobiose (0.10 ± 0.04 mM and 0.98 ± 0.26 mM). The photocatalytic activity was lower compared to direct use of glucose or cellobiose (up to 0.96 ± 0.05 $mmol_{formate}\, g_{TiO_2}^{-1}$), indicating that cellulase may somewhat inhibit photocatalytic activity. Isotopic labeling experiments confirmed $HCOO^-$ formation through both redox half reactions (Figure S9). Step-wise pre-treatment and PR formed a similar amount of 0.45 ± 0.02 $mmol_{formate}\, g_{TiO_2}^{-1}$ (Figure 4a).

Enzymatic depolymerization of cellulose does not require light irradiation and can occur in the dark without interfering with the photocatalytic step. Therefore, more practical reaction configurations were explored based on vertical illumination of the PR reactor, thereby mimicking the trajectory of natural sunlight. Using a biohybrid photocatalyst composite that can float at the solution surface, sunlight can be efficiently used for PR while different reactions not driven by light can proceed in the bulk solution, especially if a reaction suspension is involved hindering light absorption of the photocatalyst. For example, enzymatic depolymerization of cellulose can generate soluble sugar-based electron donors (dark; Figure 1b) for PR (light). This configuration will also allow for cellulose

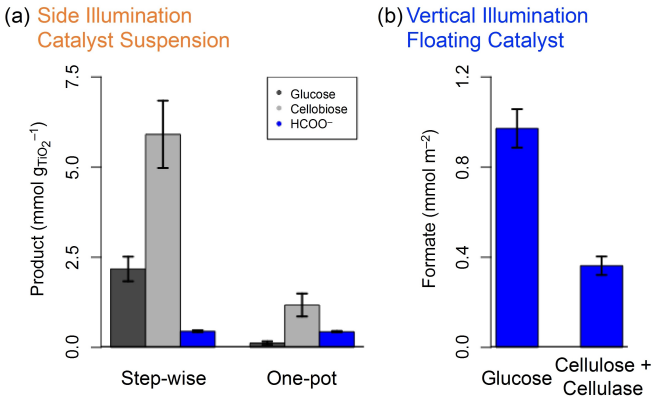

Figure 4. a) Glucose, cellobiose and formate formation after 24 h photocatalysis with TiO_2|**FDH** of a filtered cellulose suspension incubated with cellulase (step-wise) in the presence of cellulose and cellulase (one-pot). b) Floating **HGM/TiO_2**|**FDH** photocatalyst for vertical illumination combined with cellulose depolymerization with cellulase for formate formation. Reaction conditions: a) 0.83 mg TiO_2; 12 nM **FDH**; 16.2 mg cellulose; 0.8 mg cellulase; 0.1 M $NaHCO_3$; pH 6.5; 1 mL; anaerobic condition; 30 °C; 101 kPa. b) 8.3 mg **HGM/TiO_2**; 12 nM **FDH**; glucose (0.1 M) or cellulose (32.4 mg) with cellulase (1.6 mg); 0.1 M $NaHCO_3$; pH 6.5; 2 mL; anaerobic atmosphere; 30 °C; 101 kPa.

depolymerization and photocatalysis in one pot, thereby decreasing reactor footprint and solution processing.

Floating TiO_2 composites were prepared by immobilizing TiO_2 onto silica-based hollow glass microspheres (iM30k, denoted as **HGM**) using an aluminosilicate cement, denoted as **HGM/TiO$_2$** (20 wt % TiO_2; see Supporting Information for details).[34] The presence of TiO_2 (P25) was confirmed by powder XRD, SEM, UV/Vis and IR spectroscopy (see Supporting Information for details; Figures S10–S15).

PR of **HGM/TiO$_2$** was tested in a photoreactor allowing top-down irradiation (see Figure 1c, Figure S16 and Supporting Information for details) with **FDH** (2.8 $nmol_{FDH}\,g^{-1}$) self-immobilized onto **HGM/TiO$_2$** (8.3 mg) in a 0.1 M $NaHCO_3$ and 0.1 M glucose solution at pH 6.5 (Figure 4b and Table S6). After 24 h photocatalysis, 0.97 ± 0.09 $mmol_{formate}\,m^{-2}$ was formed. Isotopic labeling experiments with $^{13}CO_2/NaH^{13}CO_3$ and $^{12}C_6$-glucose, confirmed stoichiometric oxidation and reduction to $HCOO^-$ (Figure S17). Replacing glucose with cellulose and cellulase, where cellulase converted cellulose into soluble sugars in the bulk solution while photocatalysis occurred on the floating **HGM/TiO$_2$|FDH** photocatalyst generated 0.36 ± 0.04 $mmol_{formate}\,m^{-2}$ after 24 h, indicating the efficient production of $HCOO^-$.

In conclusion, we have introduced a biohybrid photocatalyst that demonstrates light-driven comproportionation of solid waste and gaseous CO_2 to produce a single energy carrier in aqueous solution under ambient temperature and pressure. The reported semiconductor-enzyme system consists of formate dehydrogenase and titanium dioxide nanoparticles (TiO_2|**FDH**), which simultaneously reduce CO_2 and oxidize various cellulose-derived wastes to formate with excellent selectivity and activity. This semi-artificial photoreforming catalyst can float when supported on low-density silica microspheres to allow for vertical illumination photocatalysis, while performing cellulose depolymerization through enzymatic pre-treatment in the dark bulk suspension. This work introduces biohybrid photoreforming catalysts to achieve full valorization of both redox reactions to form clean chemicals, which will motivate the exploration of other (bio)catalysts with improved stability and new reactivity in the future development of photoreforming.

Acknowledgements

We would like to thank the European Research Council (ERC) for a Proof of Concept Grant (SolReGen; to E.L. and E.R.) and a Consolidator Grant (MatEnSAP; to M.M. and E.R.), the Swiss National Science Foundation (Early Postdoc Fellowship: P2EZP2 191791 to E.L.) as well as the National Science and Engineering Research Council of Canada (NSERC) for a Postdoctoral Fellowship (S.L.). We thank also Fundação para a Ciência e Tecnologia (Portugal) for fellowship DFA/BD/7897/2020 (R.M.), grant PTDC/BII-BBF/2050/2020 (I.A.C.P.), MOSTMICRO-ITQB unit (UIDB/04612/2020 and UIDP/04612/2020) and Associated Laboratory LS4FUTURE (LA/P/0087/2020). Ariffin Mohamad Annuar, Subhajit Bhattacharjee, Dongseok Kim (University of Cambridge) and Victor Mougel (ETH Zürich) are acknowledged for helpful discussions.

Conflict of Interest

The authors declare no conflict of interest.

Data Availability Statement

The data that support the findings of this study are available in the Supporting Information of this article.

Keywords: Biohybrid Materials · Biomass · Carbon Dioxide Fixation · Photocatalysis · TiO_2

[1] T. Uekert, C. M. Pichler, T. Schubert, E. Reisner, *Nat. Sustain.* **2021**, *4*, 383.
[2] X. Li, J. Yu, M. Jaroniec, X. Chen, *Chem. Rev.* **2019**, *119*, 3962.
[3] A. M. Appel, J. E. Bercaw, A. B. Bocarsly, H. Dobbek, D. L. DuBois, M. Dupuis, J. G. Ferry, E. Fujita, R. Hille, P. J. A. Kenis, C. A. Kerfeld, R. H. Morris, C. H. F. Peden, A. R. Portis, S. W. Ragsdale, T. B. Rauchfuss, J. N. H. Reek, L. C. Seefeldt, R. K. Thauer, G. L. Waldrop, *Chem. Rev.* **2013**, *113*, 6621.
[4] K. E. Dalle, J. Warnan, J. J. Leung, B. Reuillard, I. S. Karmel, E. Reisner, *Chem. Rev.* **2019**, *119*, 2752.
[5] X. Yang, D. Wang, *ACS Appl. Energy Mater.* **2018**, *1*, 6657.
[6] J. L. White, M. F. Baruch, J. E. Pander, Y. Hu, I. C. Fortmeyer, J. E. Park, T. Zhang, K. Liao, J. Gu, Y. Yan, T. W. Shaw, E. Abelev, A. B. Bocarsly, *Chem. Rev.* **2015**, *115*, 12888.
[7] A. Perazio, G. Lowe, R. Gobetto, J. Bonin, M. Robert, *Coord. Chem. Rev.* **2021**, *443*, 214018.
[8] Q. Wang, K. Domen, *Chem. Rev.* **2020**, *120*, 919.
[9] A. V. Puga, *Coord. Chem. Rev.* **2016**, *315*, 1.
[10] M. F. Kuehnel, E. Reisner, *Angew. Chem. Int. Ed.* **2018**, *57*, 3290; *Angew. Chem.* **2018**, *130*, 3346.
[11] X. Wu, N. Luo, S. Xie, H. Zhang, Q. Zhang, F. Wang, Y. Wang, *Chem. Soc. Rev.* **2020**, *49*, 6198.
[12] C. Y. Toe, C. Tsounis, J. Zhang, H. Masood, D. Gunawan, J. Scott, R. Amal, *Energy Environ. Sci.* **2021**, *14*, 1140.
[13] T. Kawai, T. Sakata, *Nature* **1980**, *286*, 474.
[14] J. Schneider, M. Matsuoka, M. Takeuchi, J. Zhang, Y. Horiuchi, M. Anpo, D. W. Bahnemann, *Chem. Rev.* **2014**, *114*, 9919.
[15] D. I. Kondarides, V. M. Daskalaki, A. Patsoura, X. E. Verykios, *Catal. Lett.* **2008**, *122*, 26.
[16] Q. Xiang, J. Yu, M. Jaroniec, *J. Am. Chem. Soc.* **2012**, *134*, 6575.
[17] E. Lam, E. Reisner, *Angew. Chem. Int. Ed.* **2021**, *60*, 23306; *Angew. Chem.* **2021**, *133*, 23494.
[18] T. Reda, C. M. Plugge, N. J. Abram, J. Hirst, *Proc. Natl. Acad. Sci. USA* **2008**, *105*, 10654.
[19] A. R. Oliveira, C. Mota, C. Mourato, R. M. Domingos, M. F. A. Santos, D. Gesto, B. Guigliarelli, T. Santos-Silva, M. J. Romão, I. A. Cardoso Pereira, *ACS Catal.* **2020**, *10*, 3844.
[20] R. Sato, Y. Amao, *New J. Chem.* **2020**, *44*, 11922.
[21] R. K. Thauer, K. Jungermann, K. Decker, *Bacteriol. Rev.* **1977**, *41*, 100.
[22] C. A. R. Cotton, C. Edlich-Muth, A. Bar-Even, *Curr. Opin. Biotechnol.* **2018**, *49*, 49.

[23] C. F. Nielsen, L. Lange, A. S. Meyer, *Biotechnol. Adv.* **2019**, *37*, 107408.
[24] Y. S. Lee, R. Gerulskis, S. D. Minteer, *Curr. Opin. Biotechnol.* **2022**, *73*, 14.
[25] S. T. Stripp, B. R. Duffus, V. Fourmond, C. Léger, S. Leimkühler, S. Hirota, Y. Hu, A. Jasniewski, H. Ogata, M. W. Ribbe, *Chem. Rev.* **2022**, *122*, 11900.
[26] M. Miller, W. E. Robinson, A. R. Oliveira, N. Heidary, N. Kornienko, J. Warnan, I. A. C. Pereira, E. Reisner, *Angew. Chem. Int. Ed.* **2019**, *58*, 4601; *Angew. Chem.* **2019**, *131*, 4649.
[27] J. Wang, X. Li, M. Wang, T. Zhang, X. Chai, J. Lu, T. Wang, Y. Zhao, D. Ma, *ACS Catal.* **2022**, *12*, 6722.
[28] F. Secundo, Y. Amao, *RSC Adv.* **2020**, *10*, 42354.
[29] R. K. Yadav, G. H. Oh, N.-J. Park, A. Kumar, K.-j. Kong, J.-O. Baeg, *J. Am. Chem. Soc.* **2014**, *136*, 16728.
[30] S. Zhang, J. Shi, Y. Sun, Y. Wu, Y. Zhang, Z. Cai, Y. Chen, C. You, P. Han, Z. Jiang, *ACS Catal.* **2019**, *9*, 3913.
[31] W. W. Cleland, *Biochemistry* **1964**, *3*, 480.
[32] R. Chong, J. Li, Y. Ma, B. Zhang, H. Han, C. Li, *J. Catal.* **2014**, *314*, 101.
[33] L. Da Vià, C. Recchi, T. E. Davies, N. Greeves, J. A. Lopez-Sanchez, *ChemCatChem* **2016**, *8*, 3475.
[34] S. Linley, E. Reisner, *Adv. Sci.* **2023**, in print https://doi.org/10.1002/advs.202207314.

Manuscript received: October 28, 2022
Accepted manuscript online: March 8, 2023
Version of record online: April 12, 2023